# The Influence of Water on the Dispersion of Vanadia Supported on Silica SBA-15: A Combined XPS and Raman Study

**Christian Hess,* Genka Tzolova-Müller, and Rita Herbert**

*Department of Inorganic Chemistry, Fritz Haber Institute of the Max Planck Society, Faradayweg 4-6, 14195 Berlin, Germany*

*Received: February 19, 2007; In Final Form: April 13, 2007*

The influence of water on the dispersion and structure of silica SBA-15-supported vanadia model catalysts has been studied using X-ray photoelectron spectroscopy (XPS) and Raman spectroscopy, which were combined within one experimental setup, as well as UV−vis diffuse reflectance spectroscopy. By performing time-dependent XPS experiments, the influence of UHV/X-ray radiation could be eliminated by extrapolation of the observed temporal changes to $t = 0$. XPS characterization reveals that the $V2p_{3/2}$ emission consists of two contributions, which are assigned to vanadia with distinctly different cluster size. Dehydration by treatment in oxygen flow at elevated temperatures leads to a significant increase in total intensity and a substantial redistribution of spectral weight to higher binding energies as a result of an increase in the vanadia dispersion. The V/Si XPS intensity ratio of the dehydrated samples closely follows the corresponding bulk ratio over the whole range of vanadium loadings (0−22 wt % V) studied. This observation renders possible a correlation of XPS and Raman results allowing for quantification of Raman features such as the relative cross sections of the vanadyl surface species. It is shown that the observed changes in vanadia dispersion are directly associated with the changes in the molecular structure of the surface vanadia species.

## Introduction

Supported vanadium oxide catalysts exhibit a large potential for a variety of oxidation reactions such as the selective oxidation of methane and methanol to formaldehyde and the oxidative dehydrogenation of ethane and propane.[1] However, despite extensive research, there are still fundamental aspects of supported metal oxide catalysts, which have not been addressed in the literature adequately to their importance, such as carbon deposition and changes in catalyst dispersion during reaction.[2] Water is a common product of selective oxidation reactions of alkanes. In addition, water vapor is often added to the feed to improve the catalyst performance. The conditions of operation allow for hydrothermal reactions involving oxolation and olation processes leading to polymerization/depolymerization of an initial $V_xO_y$ condensate. It is known from the literature that the structure of the fully hydrated state of silica-supported vanadia species closely resembles $V_2O_5 \cdot nH_2O$ gels with vanadium in pseudo-octahedral coordination forming layers of two-dimensional polyvanadates.[3−5] Dehydrated vanadia at low V coverages, i.e., below the coverage at which $V_2O_5$ is formed, has been proposed to be present as isolated tetrahedral $VO_4$.[4−6] However, in recent FT-IR experiments on silica SBA-15-supported vanadium oxide using NO as probe molecule, the formation of V-bonded bridged nitrates was observed implying the presence of dimers and/or polymers.[7] This observation is consistent with a recent experimental and theoretical model catalyst study on alumina and silica-supported vanadia, which has shown that the Raman feature observed around 950 $cm^{-1}$ for the alumina system is due to an Al−O−V interface mode rather than V−O−V vibrations as has been suggested in the literature.[8] Regarding the silica system, which does not show a Raman band in the 950 $cm^{-1}$ region, the absence of that band therefore neither proves nor excludes the presence of V−O−V.

It has been shown that the dispersion of supported metal oxides catalysts can be determined by measuring the oxygen uptake of the reduced active phase (e.g., vanadium oxide) in an oxygen chemisorption experiment.[9] This indirect method allows for evaluation of the fraction of accessible active phase atoms, but results may be complicated by the uncertainty of the extent of reduction and restructuring of the active phase. In contrast, XPS can provide direct information on the dispersion of supported metal oxide catalysts[10] such as vanadia supported on $SiO_2$, $Al_2O_3$,[11] and $TiO_2$.[12] Interestingly, in previous XPS studies on silica-supported vanadia catalysts and vanadia-silica mixed oxide systems vanadium species with $V2p_{3/2}$ binding energies of up to 2 eV higher compared to those of reference compounds such as $V_2O_5$ were found, which were attributed to vanadium species strongly interacting with silica.[13−17] However, the above studies were performed on samples exposed to air before being introduced into the XPS chamber without further treatment. Despite the well-known influence of water, XPS has only recently been applied to study the effect of dehydration on the vanadia dispersion.[18]

The combination of spectroscopic techniques within one setup to study the same sample offers the advantage to obtain spectroscopic results which can be directly correlated, as any influence of both the particular sample and the reaction cell geometry, which may affect the heating and gas flow conditions, is removed. Combining XPS with Raman spectroscopy is of particular interest for the characterization of heterogeneous catalysts as these methods provide complementary information. Whereas Raman spectroscopy provides bulk information on the catalyst structure, XPS can give access to the composition, oxidation state(s) and dispersion of the surface region of the

* Corresponding author. E-mail: hess@fhi-berlin.mpg.de.

10.1021/jp0713920 CCC: $37.00 
Published on Web 06/02/2007

**TABLE 1: BET Characteristics of the Synthesized SBA-15-Supported Vanadium Oxides Compared to the Blank SBA-15 Support**

| | $V$ (wt %) | $V$ ($nm^2$) | $V$ (mmol/g) | $S_{BET}$ ($m^2/g$) | $d_p$ (nm) | $V_p$ (mL/g) |
|---|---|---|---|---|---|---|
| SBA-15 | 0.0 | 0.0 | 0.0 | 897 | 7.0 | 1.1 |
| SBA-15 (ox) | 0.0 | 0.0 | 0.0 | 408 | 6.2 | 0.5 |
| 2.7 wt % V/SBA-15 | 2.7 | 0.7 | 0.53 | 445 | 6.7 | 0.5 |
| 5.4 wt % V/SBA-15 | 5.4 | 1.4 | 1.05 | 440 | 6.6 | 0.5 |
| 10.8 wt % V/SBA-15 | 10.8 | 4.7 | 2.12 | 273 | 5.5 | 0.3 |
| 21.9 wt % V/SBA-15 | 21.9 | 47 | 4.30 | 55 | 4.8 | 0.1 |
| 3.6 wt % V/SBA-15 (im) | 3.6 | 0.7 | 0.71 | 646 | 6.8 | 0.8 |

catalyst. Previously, Raman spectroscopy has been combined with FT-IR, UV−vis, EPR and ED-XAFS as summarized in a recent review article.[19]

For a detailed understanding of catalyst properties, the use of materials with well-defined structure is necessary. To proceed in this direction, we have prepared vanadium oxide model catalysts via controlled grafting/anion exchange, which consists of functionalization of SBA-15, subsequent anion exchange of decavanadate into the pores of the silica matrix and thermolysis of the precursor material. As the precursor is tightly held electrostatically within the channels in a prearranged geometry, this approach allows to precisely control the amount of vanadium introduced into the material over a broad range of vanadia loadings (0-22 wt % V).[20,21] Hence, due to its well-defined preparation and structure, this vanadia model catalyst seems very well suited as a three-dimensional model system to give new insights into the nature of the active site as well as the relation between structure and activity in partial oxidation reactions.[22] Only recently, we have demonstrated the catalytic properties of this catalyst system in the propane partial oxidation to acrylic acid as well as methanol partial oxidation to formaldehyde.[23,24]

As part of our strategy for understanding the properties of silica-supported vanadia in detail, we intend to bridge the gap between well-defined powder and planar model systems. As planar reference samples, surface science models of silica-supported vanadium oxide catalysts have been prepared by spin-coating impregnation. These chemically prepared planar systems allow for a close link to the well-defined and well-studied model systems prepared by physical methods.[8]

In this contribution, a combined XPS and Raman study of the changes associated with the transformation of the fully hydrated catalyst into its more dispersed dehydrated state is presented. We observed dramatic changes in the photoelectron spectra of supported vanadium oxide powder catalysts upon dehydration, which can be directly related to changes in the catalyst dispersion and surface structure. The focus of our study is vanadia supported by mesoporous silica SBA-15 with vanadium loadings ranging from 2.7 wt % V, at which no $V_2O_5$ is present, up to 22 wt % V, at which $V_2O_5$ represents a significant fraction of the vanadia in the catalyst.

## Experimental Section

**1. Catalyst Preparation.** Details of the catalyst preparation are described elsewhere.[20] Briefly, functionalization of SBA-15 was achieved by adding 3-aminopropyltrimethoxysilane (APTMS) to a suspension of SBA-15 in toluene at 65 °C. After stirring for 12 h, the contents were filtered, washed, and finally stirred in 0.3 M HCl for 12 h. For SBA-15-supported vanadium oxide catalysts (V/SBA-15), appropriate amounts of butylammonium decavanadate were added to a suspension of functionalized SBA-15 in water. The resulting powder was calcined at 550 °C for 12 h. A SBA-15 reference sample, denoted as SBA-15 (ox), was prepared according to the above procedure, however, in the ion-exchange step potassium oxalate monohydrate (Fluka, >99.5%) instead of decavanadate was used.

Two reference samples with the same vanadium concentration (0.7 V/$nm^2$) as 2.7 wt % V/SBA-15 (see Table 1) were prepared. The first sample, denoted as V/SBA-15 (im), is a SBA-15-supported vanadium oxide sample prepared in a glovebox by incipient wetness impregnation using a 2-propanol solution of vanadium isopropoxide ($VO(O-Pr_i)_3$, Alfa Aesar, 95−99% purity). The sample was dried in He flow at 120 °C for 1 h and at 300 °C for 2 h. Finally, the sample was calcined in air at 550 °C for 2 h. The second sample, denoted as $V/SiO_2/Si$ (im), was prepared on a flat Si(100) wafer via spin-coating impregnation adopting the procedure developed by Thüne et al.[25] for the preparation of silica-supported chromia to vanadia. The silicon wafers were calcined in air at 800 °C to form an amorphous silica overlayer. The calcined samples were rehydroxylated in boiling water for 1 h and finally dried in air overnight. Spin-coating was performed in air at 2800 rpm using a 2-propanol solution of vanadium isopropoxide. After impregnation the sample was calcined in air at 550 °C for 2 h. The V loading was determined based on the model by Hardeveld et al.[26]

The hydrated samples studied were in their fully hydrated state in air at room temperature. They were obtained by exposing the as prepared samples to ambient for 2 months. Dehydrated samples were prepared by treatment in 20% $O_2$/He (50 mL/min) at 300 °C for 60 min and subsequent cooling to room temperature.

**2. Physical Characterization.** The vanadium content of the catalyst samples was determined by ICP-AES (inductively coupled plasma atomic emission spectroscopy). Surface areas of the prepared samples were measured by nitrogen adsorption/desorption isotherms and standard multipoint BET analysis methods. The pore volume was determined from the adsorption branch of the $N_2$ isotherm curve at the $P/P_0 = 0.95$ signal point. The pore-size distribution was calculated from the isotherm using the NLDFT method.

**3. Combined XPS and Raman setup.** The measurements were carried out using a modified LHS/SPECS EA200 MCD system equipped with a Mg $K_\alpha$ source (1253.6 eV, 168 W). The first evacuation cell of this XPS apparatus was modified to allow for sample pretreatment using continuous gas flow as well as a Raman fiber probe to be inserted into the cell for in situ Raman studies. The powder samples were placed as is in a stainless steel sample holder with a 0.6 mm deep rectangular well covering an area of $(12 \times 8)$ $mm^2$. For each sample, first a Raman spectrum and then XP spectra were recorded. All spectra were recorded at room temperature. After the Raman experiments the samples were transferred to the XPS analysis chamber without exposure to air (quasi in situ). Raman spectra were recorded with a fiber probe using 514 nm laser excitation (5 mW) of an argon ion laser (Melles Griot) at 5 $cm^{-1}$ spectral resolution (Kaiser Optical, HL5R with CCD). Sampling times

**TABLE 2: Atomic Ratios (%) of the Detected Elements of the Synthesized SBA-15-Supported Vanadium Oxides and Blank SBA-15 as Obtained from the XPS Analysis**

| | O1s | V2p$_{3/2}$ | C1s | Si2p | V/Si |
|---|---|---|---|---|---|
| SBA-15 (hydr) | 69.4 | | 0.6 | 30.0 | |
| SBA-15 (dehydr) | 70.2 | | 0 | 29.8 | |
| SBA-15 (ox) (hydr) | 69.1 | | 0.7 | 30.2 | |
| SBA-15 (ox) (dehydr) | 70.3 | | 0 | 29.7 | |
| 2.7 wt % V/SBA-15 (hydr) | 70.1 | 0.7 | 0.7 | 28.5 | 0.025 |
| 2.7 wt % V/SBA-15 (dehydr) | 68.2 | 1.0 | 0.8 | 30.0 | 0.032 |
| 5.4 wt % V/SBA-15 (hydr) | 68.2 | 1.5 | 1.3 | 29.0 | 0.052 |
| 5.4 wt % V/SBA-15 (dehydr) | 68.3 | 2.3 | 0.4 | 29.0 | 0.078 |
| 10.8 wt % V/SBA-15 (hydr) | 70.5 | 2.4 | 0.9 | 26.2 | 0.092 |
| 10.8 wt % V/SBA-15 (dehydr) | 67.8 | 4.1 | 0.5 | 27.6 | 0.149 |
| 21.9 wt % V/SBA-15 (hydr) | 67.6 | 5.8 | 1.9 | 24.7 | 0.236 |
| 21.9 wt % V/SBA-15 (dehydr) | 66.7 | 7.5 | 1.1 | 24.7 | 0.304 |
| 3.6 wt % V/SBA-15 (im) (hydr) | 70.0 | 0.8 | 1.0 | 28.2 | 0.027 |

were typically 30 min. The binding energy scale of the XPS system was calibrated using Au4f$_{7/2}$ = 84.0 eV and Cu2p$_{3/2}$ = 932.67 eV from foil samples. The base pressure of the ultrahigh vacuum (UHV) chamber was $1 \times 10^{-10}$ mbar. During the XPS experiments, the pressure increased to about $1 \times 10^{-9}$ mbar. Data acquisition time was 100 min. To account for the effect of UHV/X-ray induced changes on the XP spectra, series of spectra as a function of time were recorded. The temporal changes of the contributions of the V2p$_{3/2}$ components can be well described by a first-order exponential decay/growth and were used to determine their values at $t = 0$. Charging of the powder samples was accounted for by setting the peak of the Si2p signal to 103.6 eV.[27,21] For the hydrated (air-exposed) samples, the C1s signal from adventitious carbon was located at 284.7 eV, in excellent agreement with the common reference value of 284.7 ± 0.5 eV.[27] Further data reduction included satellite deconvolution and subtraction of a Shirley background. Quantitative data analysis was performed on the basis of peak areas by fitting with 30/70 Gauss-Lorentz product functions. Atomic ratios were calculated using empirical cross sections.[28]

**4. UV−Vis Diffuse Reflectance Spectroscopy.** Diffuse reflectance UV−vis spectra were measured with a Perkin-Elmer Lambda 950 spectrometer equipped with a Harrick diffuse reflectance attachment. Samples were dehydrated in 50% $O_2$/$N_2$ (20 mL/min) at 300 °C for 1/2 h before measuring spectra at room temperature. The Kubelka−Munk function (F(R∞)) was used to convert diffuse reflectance data into absorption spectra using Spectralon as a standard.

## Results

**Physical Characterization.** The results of the $N_2$ physisorption analysis of the SBA-15- and the SBA-15-supported vanadium oxide samples are given in Table 1. As discussed previously, the hexagonal structure of SBA-15 is preserved in the presence of vanadia.[20] With the deposition of vanadium oxide, the surface area ($S_{BET}$), pore diameter ($d_p$), and pore volume ($V_p$) shift to lower values, which suggests that the vanadia species are located inside the pores of SBA-15, coating the inner walls of the mesoporous matrix.[20] However, physisorption data also reveal that in the presence of surface vanadia, the mesoporous channels remain accessible for reactants. At higher loadings (>5.4 wt % V), a strong decrease in surface area is observed. As discussed below, the Raman results show that for the 10.8 wt % and 21.9 wt % V/SBA-15 samples, 3-dimensional $V_2O_5$ crystallites are present. Thus, the smaller surface areas at higher loadings are most probably caused by channel blocking. The lower surface area of 2.7 wt % V/SBA-15 compared to 3.6 wt % V/SBA-15 (im) (see Table 1) is a result of the organofunctionalization of SBA-15 in the course of the multistep preparation procedure.[20,21]

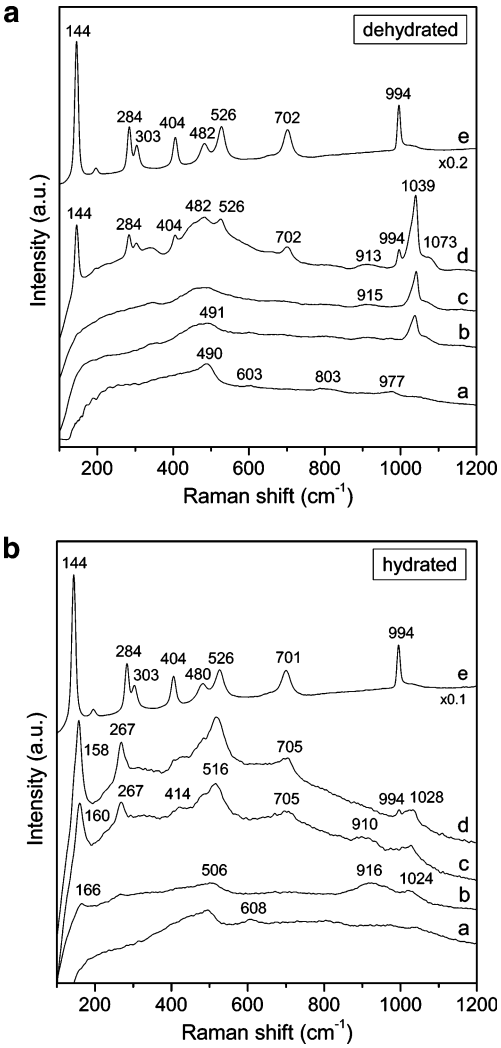


**Figure 1.** Raman spectra of dehydrated (top) and hydrated (bottom) SBA-15-supported vanadia as well as blank SBA-15 (ox). The vanadium loadings are (a) 0, (b) 2.7, (c) 5.4, (d) 10.8, and (e) 21.9 wt % V. The spectra are offset for clarity.

The atomic ratios of the detected elements, as obtained from the XPS analysis, as well as the corresponding V/Si ratios are listed in Table 2. For the SBA-15 samples, oxygen, carbon, and silicon were detected. Besides carbon, the deposition of vanadium oxide does not lead to the introduction of any other impurities. Also, there is no significant increase in the amount of carbon for the SBA-15-supported vanadia samples compared to the SBA-15 samples. These results indicate that during the calcination step essentially all organic residues, which were introduced during the functionalization of SBA-15, were removed.[21] As expected, treatment in oxygen led to a reduction of the amount of carbon.

**Raman Spectra**. The top panel of Figure 1 depicts the Raman spectra of SBA-15 (ox) and SBA-15-supported vanadia in their dehydrated state. The Raman spectrum of SBA-15 (ox) is shown as reference as small differences were observed compared to that of untreated SBA-15. The spectrum of SBA-15 (ox) (spectrum a) is characterized by an intense Raman feature around 490 cm$^{-1}$ as well as weaker features at 603, 803, and 977 cm$^{-1}$. The 490 cm$^{-1}$ band can be assigned to cyclic tetrasiloxane rings of the silica support (D1 defect mode).[29] The weaker Raman bands at 603, 803 and 977 cm$^{-1}$ are attributed

to cyclic trisiloxane rings (D2 defect mode), the symmetrical Si−O−Si stretching mode and the Si−OH stretch of surface hydroxyl groups, respectively.[29,30] Upon loading of vanadia onto SBA-15, new Raman bands appear around 915 and 1039 $cm^{-1}$ (spectra b and c). The Raman band around 1039 $cm^{-1}$ has an asymmetric band shape with a shoulder at 1073 $cm^{-1}$.[31] It is assigned to the V═O stretch vibration of tetrahedrally coordinated V ions of predominanly small aggregates of polymerized $VO_4$ units.[7] The features at 915 $cm^{-1}$ can either be due to vibrations of the surface vanadia species or changes related to the silica surface upon grafting of vanadia. As the Raman band at 1073 $cm^{-1}$ is observed only after deposition of vanadia it can either be due to vibrations of the surface vanadia species and/or changes related to the silica surface upon grafting of vanadia such as the formation of $Si-O^-$ and $Si(-O^-)_2$ functionalities.[32]

With increasing vanadium loading (spectrum d) the intensity of the 1039 $cm^{-1}$ vanadyl band strongly increases. Moreover, new bands appear at 144, 284, 303, 404, 482, 526, 702, and 994 $cm^{-1}$, which are typical for crystalline $V_2O_5$. The latter bands dominate the spectrum at the highest loading (spectrum e).

The bottom panel of Figure 1 shows the Raman spectra of SBA-15 (ox) and SBA-15-supported vanadia in their fully hydrated state under ambient conditions. The spectrum of hydrated SBA-15 (ox) (spectrum a) resembles that of dehydrated SBA-15 (ox), however the feature at 977 $cm^{-1}$ is less pronounced. Deposition of vanadia leads to the appearance of broad Raman bands around 916 and 1024 $cm^{-1}$ (spectrum b). At higher vanadium loading (spectrum c), additional bands are observed at 160, 267, 414, 516 and 705 $cm^{-1}$. Spectrum c shows some similarity with that of crystalline $V_2O_5$, however, additional bands at 267 and 1024 $cm^{-1}$ are present. The spectrum is in good agreement with previously recorded spectra of hydrated vanadia supported by silica.[4,5] It resembles the Raman spectra of the xerogels $V_2O_5 \cdot nH_2O$ studied by Abello et al.[33,34] At a vanadium loading of 10.8 wt % V (spectrum d), an additional feature at 994 $cm^{-1}$ is observed which indicates the presence of some $V_2O_5$. At the highest loading (spectrum e), the spectrum is dominated by bands typical for crystalline $V_2O_5$ resembling the situation of the corresponding dehydrated sample.

**UV−Vis Diffuse Reflectance Spectra.** UV−vis spectra of dehydrated and hydrated V/SBA-15 are shown in the top and bottom panel of Figure 2, respectively. Both sets of spectra exhibit broad oxygen → vanadium charge-transfer (CT) bands. It is known from the literature that the position of the CT bands is a sensitive indicator for the vanadium coordination and the degree of polymerization of the vanadium oxide species.[3,5] For the dehydrated samples with low vanadium loading (≤5.4 wt % V), one absorption band in the UV region at ∼260 nm is observed. At higher loadings (10.8 wt % V), this band broadens and exhibits an additional absorption tail, which extends into the visible region of the spectrum up to ∼500 nm. For 21.9 wt % V/SBA-15, a significant increase in the absorption around 400 nm and the intensity ratio of the bands at 370 and 260 nm is observed. Note that at the highest loading sample absorption leads to a noticeable decrease in the overall intensity of the diffusively reflected light as compared to the 10.8 wt % V sample. All hydrated samples show a similar absorption behavior, which is characterized by a UV absorption band at ∼260 nm and a band at ∼370 nm with an absorption tail extending into the visible region. For the sample with the highest loading (21.9 wt % V), as in the dehydrated case, an increase in the intensity ratio of the bands at 370 and 260 nm is observed.

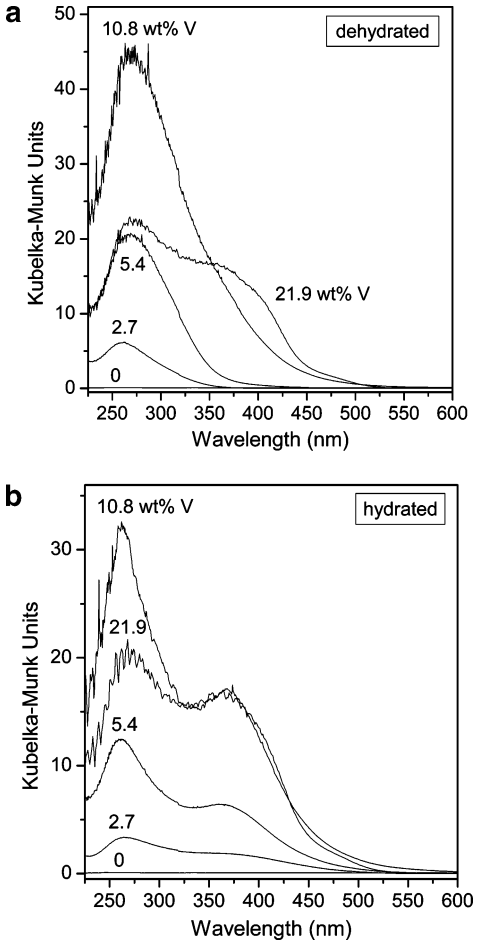


**Figure 2.** UV−vis diffuse reflectance spectra of dehydrated (top) and hydrated (bottom) SBA-15-supported vanadia as well as blank SBA-15. The vanadium loadings are (a) 0, (b) 2.7, (c) 5.4, (d) 10.8, and (e) 21.9 wt % V.

Previously, UV−vis absorption bands of supported vanadia catalysts were assigned by comparison with those of vanadium reference compounds.[3,5,20] Absorption bands with maxima at around 250/290 nm and at around 280 nm were ascribed to tetrahedrally coordinated isolated and dimeric vanadates, respectively. Band maxima at 288/363 nm ($NH_4VO_3$) and at 281/353 nm ($NaVO_3$) were assigned to tetrahedrally coordinated polyvanadate, respectively.[5] Crystalline $V_2O_5$ shows UV−vis absorption over a broad spectral range (∼220−600 nm) with a maximum in intensity at around 420 nm. Therefore, the spectra of the dehydrated samples at loadings ≤5.4 wt % V suggest the presence of tetrahedrally coordinated vanadium, whereas at higher loadings (10.8 wt % V) a small amount of $V_2O_5$ or pentahedrally coordinated vanadium is present. The appearance of a Raman feature at 994 $cm^{-1}$ for 10.8 wt % V/SBA-15 (see Figure 1) confirms the presence of crystalline $V_2O_5$. For the 21.9 wt % V sample the stronger absorption above 400 nm indicates the presence of a significant fraction of $V_2O_5$ crystallites in agreement with the intensity increase of the Raman band at 994 $cm^{-1}$. Hydration of the samples leads to very similar UV−vis spectra with absorption bands at around 260 and 370 nm at all loadings indicating the presence of polymerized vanadium oxide species consistent with the Raman results.

**X-Ray Photoelectron Spectra.** Figure 3 depicts a detailed XP spectrum of the $V2p_{3/2}$ region of 2.7 wt % V/SBA-15 (spectrum b), together with the corresponding spectrum of blank SBA-15 (spectrum a) after satellite subtraction. As the spectrum of SBA-15 shows structure in the V2p region due to inadequate

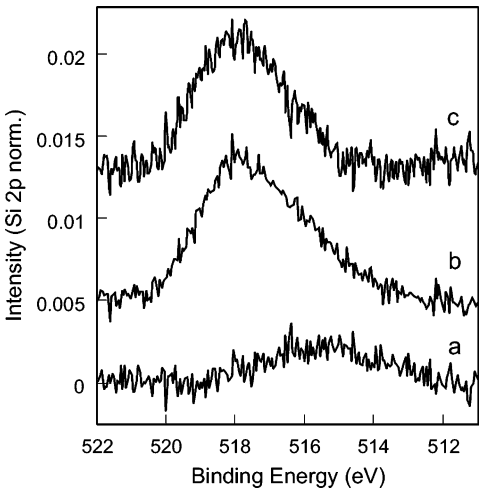


**Figure 3.** XP spectra of (a) blank SBA-15 and (b) 2.7 wt % V/SBA-15. The resulting background-subtracted spectrum of 2.7 wt % V/SBA-15 is shown as spectrum c. The spectra are offset for clarity.

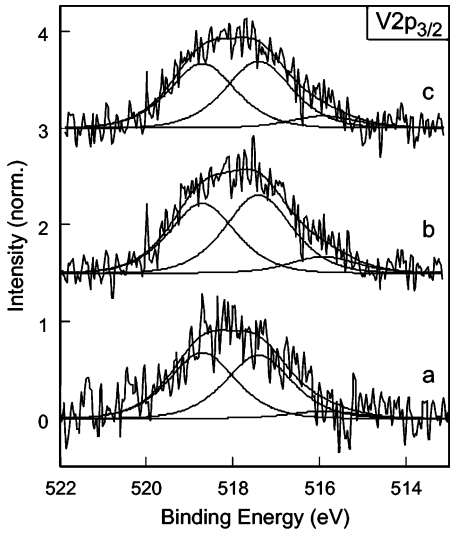


**Figure 4.** XP $V2p_{3/2}$ spectra of (a) $V/SiO_2/Si$ (im), (b) 3.6 wt % V/SBA-15 (im), and (c) 2.7 wt % V/SBA-15, together with least-square fits to the data. The spectra are offset for clarity. For details see text.

removal of the $K\alpha_5$ satellite of the nearby O1s line, it was used for background subtraction. The resulting spectrum is shown on the top of Figure 3 (spectrum c). The same procedure was applied to all other XP raw spectra.

The influence of charging and sample preparation on the XP spectra was studied using two reference samples with the same vanadium concentration (0.7 $V/nm^2$) as 2.7 wt % V/SBA-15. Figure 4 shows the normalized XP spectra of the $V2p_{3/2}$ region of $V/SiO_2/Si$ (im) (spectrum a), 3.6 wt % V/SBA-15 (im) (spectrum b), and 2.7 wt % V/SBA-15 (spectrum c), together with the least-square fits to the data. For quantitative analysis the data was deconvoluted into three peaks with binding energies at 518.7, 517.4 and 515.9 eV, respectively, and a constant fwhm (2.0 eV). The results of the peak-fitting analysis are summarized in Table 3. The $V/SiO_2/Si$ (im) sample represents a surface science model of silica-supported vanadium oxide for which charging is largely removed.[35] The $V2p_{3/2}$ signal of $V/SiO_2/Si$ (im) strongly resembles that of the 2.7 wt % V/SBA-15 powder catalyst regarding position, width and intensity distribution. Thus it is reasonable to conclude that charging does not have a significant effect on the $V2p_{3/2}$ emission of the V/SBA-15 powder samples studied. Also, comparison of the $V2p_{3/2}$ signal of 2.7 wt % V/SBA-15 with that of 3.6 wt % V/SBA-15 (im),

**TABLE 3: Results of the $V2p_{3/2}$ Analysis of SBA-15- and $SiO_2$/Si-Supported Vanadium Oxides**

| | position (eV) | width (eV) | % |
|---|---|---|---|
| $V/SiO_2/Si$ (im) | 518.7 | 2.0 | 48.4 |
| (hydr) | 517.4 | 2.0 | 46.4 |
| | 515.9 | 2.0 | 5.2 |
| 3.6 wt % V/SBA-15 (im) | 518.7 | 2.0 | 42.4 |
| (hydr) | 517.4 | 2.0 | 47.6 |
| | 515.9 | 2.0 | 10.0 |
| 2.7 wt % V/SBA-15 | 518.7 | 2.0 | 45.0 |
| (hydr) | 517.4 | 2.0 | 46.6 |
| | 515.9 | 2.0 | 8.4 |

which was prepared by impregnation of a 2-propanol solution of vanadium isopropoxide onto SBA-15 confirms that the preparation procedure has no noticeable influence on the position and shape of the $V2p_{3/2}$ spectrum.

Figure 5 shows the normalized Si2p (left) and O1s (right) emission of 2.7 wt % V/SBA-15 in its hydrated (spectrum a) and dehydrated (spectra b) state. For the other V/SBA-15 samples, similar results were obtained. Small changes in the peak width and position, but no changes in the peak shape were observed. Quantitative analysis shows that the Si2p spectrum of the dehydrated sample (fwhm: 2.6 eV) exhibits a slightly larger width than the hydrated sample (fwhm: 2.5 eV), respectively. The O1s spectrum of the dehydrated sample is slightly shifted to higher BE values. Similar changes in the Si2p and O1s spectra have been explained by different contributions to differential charging.[36] However, as demonstrated above (see Figure 4) such differences do not have a noticeable influence on the shape of the $V2p_{3/2}$ spectra.

The top panel of Figure 6 shows the $V2p_{3/2}$ spectra of 2.7 wt % V/SBA-15 and 5.4 wt % V/SBA-15 in their hydrated (spectra a and c) and dehydrated (spectra b and d) state, together with a least-square fit to the data. For clarity, the corresponding $V2p_{3/2}$ spectra of 10.8 wt % V/SBA-15 and 21.9 wt % V/SBA-15 are depicted in the bottom panel of Figure 6. As no noticeable change of the XP spectra and Raman spectra was observed over several months, we conclude that the hydrated spectra shown correspond to the fully equilibrated state of silica-supported vanadia in air at room temperature. Upon dehydration a significant increase in total intensity and a substantial redistribution of spectral weight to higher binding energies (BE) are observed. The extent of these changes in the XP spectra was dependent on the treatment conditions.[37]

Quantitative analysis was performed using three fit functions. The results from the peak-fitting analysis are summarized in Table 4.[38] By recording time-dependent XP spectra, the effect of UHV/X-ray induced changes was accounted for and the corresponding contributions of the $V2p_{3/2}$ components at $t = 0$ min could be determined (see experimental). For the lowest vanadium loading (2.7 wt % V), the analysis yields an intensity increase of the band at 518.8 eV from 41% to 83% upon dehydration. Similarly, the band centered at 517.4 eV shows an intensity decrease from 58% to 17%. For the 5.4 wt % V sample, dehydration leads to an intensity increase of the band around 518.8 eV from 43% to 89.5%, while the band centered at 517.5 eV shows an intensity decrease from 56% to 10.5%. Comparison with literature data on $V2p_{3/2}$ binding energies (BE) for binary vanadium oxides and supported vanadium oxide powder materials allows assigning the bands at 515.9 and 517.4 eV to $V^{3+}$ and $V^{5+}$, respectively.[39,40] The band at 518.8 eV is attributed to the highly dispersed vanadium oxide as will be discussed below. Note that the widths of the three fit functions used for quantitative analysis (see Table 4) are lower than those used to describe well-ordered vanadia films[41]

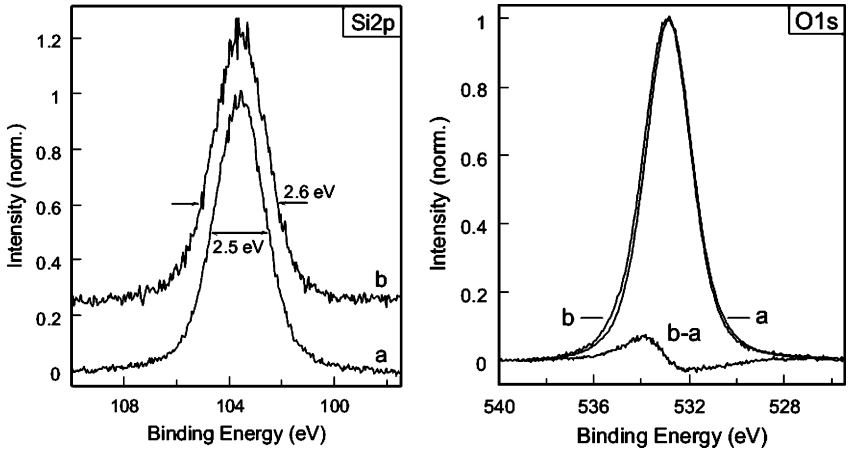


**Figure 5.** Left panel: XP Si2p spectra of (a) hydrated (b) dehydrated 2.7 wt % V/SBA-15. Spectra are offset for clarity. Right panel: XP O1s spectra of (a) hydrated and (b) dehydrated 2.7 wt % V/SBA-15 as well as the difference spectrum (b − a).

confirming the homogeneity of our powder model system. The above assignment is fully consistent with the results of the time-dependent analysis, which have shown an increase in intensity around 515.9 eV with time due to UHV/X-ray induced reduction of the vanadia samples. As room-temperature EPR experiments on dehydrated 2.7 wt % V/SBA-15, which was pretreated according to the protocol described in the experimental section, showed no $V^{4+}$ signal and those on hydrated 2.7 wt % V/SBA-15 gave a $V^{4+}$ signal corresponding to only 0.3% of the total amount of V, the quantitative analysis was restricted to $V^{5+}$ and $V^{3+}$ species.

The changes in the $V2p_{3/2}$ emission upon dehydration of 10.8 wt % V/SBA-15 (depicted in Figure 6) strongly resemble the behavior discussed above. The analysis yields an intensity increase of the band around 518.7 eV from 54% to 97% (see Table 4). Likewise, the band centered at 517.5 eV shows an intensity decrease from 45% to 3%. For the sample with the highest loading (21.9 wt % V), the overall shape of the $V2p_{3/2}$ emission looks quite different, which results from the presence of a significant amount of $V_2O_5$ as suggested by the Raman results. However, the increase in total intensity and redistribution of spectral weight to higher BE on dehydration are still observed.

Figure 7 shows the O1s spectra of SBA-15 and SBA-15-supported vanadia samples in their hydrated and dehydrated state together with a least-square fit to the data. The O1s spectra of 2.7 wt % V/SBA-15 are not included as they strongly resemble those of 5.4 wt % V/SBA-15. The results from the peak-fitting analysis are summarized in Table 5. The O1s spectra are dominated by a band around 532.9 eV, which can readily be assigned to oxygen of the silica support.[27] Besides, the O1s spectra of the V/SBA-15 samples show a contribution around 530.5 eV, which is due to oxygen in the surface vanadia species. For the 21.9 wt % V/SBA-15 samples, the O1s emission at 530.5 eV constitutes a significant contribution to the overall O1s intensity. It can be assigned to oxygen in $V_2O_5$ by comparison with the literature and considering the fact that the Raman spectra for the 21.9 wt % V/SBA-15 sample clearly show the presence of $V_2O_5$.[41] Please note that based on the value of the O1s BE only no decision about the presence of a particular binary vanadium oxide can be made as for $V_2O_3$, $V_2O_4$, and $V_2O_5$ BE values within 529.7−530.3 eV were reported.[39] On the basis of the $V2p_{3/2}$ contribution at 517.4 eV and the O1s contribution at 530.5 eV, the V/O ratio is determined to be 0.42 (0.40) for dehydrated (hydrated) 21.9 wt % V/SBA-15. This value is in excellent agreement with the value of 0.4 expected for $V_2O_5$ and therefore nicely confirms the above assignment.

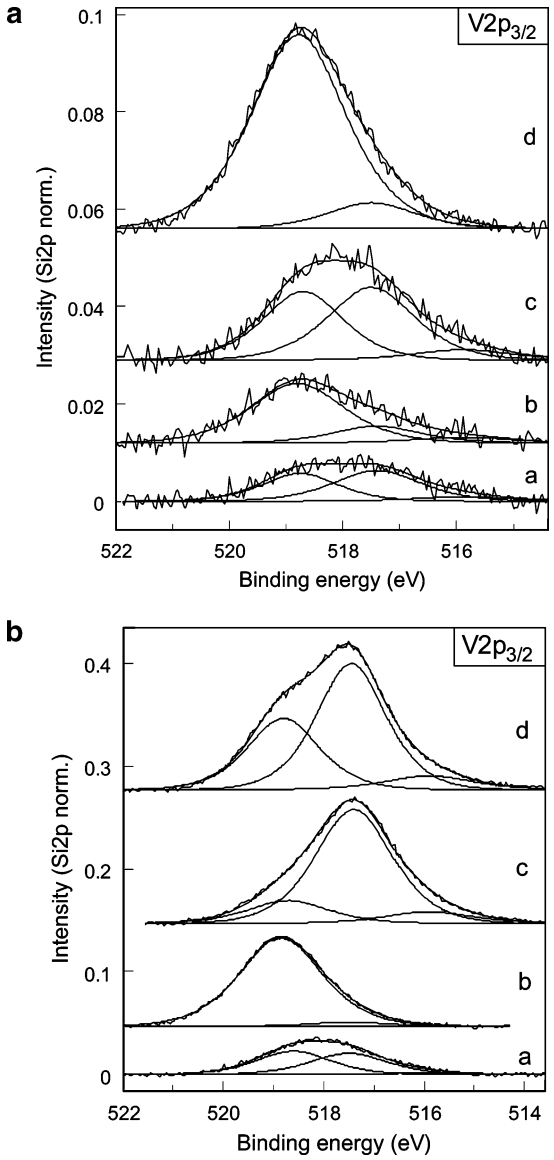


**Figure 6.** Top panel: XP $V2p_{3/2}$ spectra of (a) hydrated 2.7 wt % V/SBA-15, (b) dehydrated 2.7 wt % V/SBA-15, (c) hydrated 5.4 wt % V/SBA-15, and (d) dehydrated 5.4 wt % V/SBA-15 together with the least-square fits to the data. Bottom panel: XP $V2p_{3/2}$ spectra of (a) hydrated 10.8 wt % V/SBA-15, (b) dehydrated 10.8 wt % V/SBA-15, (c) hydrated 21.9 wt % V/SBA-15, and (d) dehydrated 21.9 wt % V/SBA-15, together with the least-square fits to the data. The spectra are offset for clarity. For details, see text.

**TABLE 4: Results of the V2p$_{3/2}$ Analysis of SBA-15-Supported Vanadium Oxides**

| | position (eV) | width (eV) | % ($t$ = 100 min) | % ($t$ = 0 min) |
|---|---|---|---|---|
| 2.7 wt % V/SBA-15 | 518.8 | 1.8 | 40.4 | 41.2 |
| (hydr) | 517.4 | 2.0 | 51.3 | 58.4 |
| | 515.9 | 2.2 | 8.3 | 0.4 |
| 2.7 wt % V/SBA-15 | 518.8 | 2.1 | 73.6 | 83.1 |
| (dehydr) | 517.4 | 2.0 | 19.1 | 16.9 |
| | 515.9 | 2.2 | 7.3 | 0 |
| 5.4 wt % V/SBA-15 | 518.7 | 1.8 | 43.0 | 42.8 |
| (hydr) | 517.5 | 2.0 | 49.2 | 55.9 |
| | 515.9 | 2.2 | 7.8 | 1.3 |
| 5.4 wt % V/SBA-15 | 518.8 | 2.1 | 88.7 | 89.5 |
| (dehydr) | 517.5 | 2.0 | 11.0 | 10.5 |
| | 515.9 | 2.2 | 0.3 | 0 |
| 10.8 wt % V/SBA-15 | 518.6 | 2.0 | 49.5 | 53.8 |
| (hydr) | 517.5 | 2.0 | 46.7 | 45.1 |
| | 515.9 | 2.2 | 3.8 | 1.1 |
| 10.8 wt % V/SBA-15 | 518.8 | 2.1 | 95.8 | 96.6 |
| (dehydr) | 517.5 | 2.0 | 4.2 | 3.4 |
| | 515.9 | 2.2 | 0 | 0 |
| 21.9 wt % V/SBA-15 | 518.7 | 2.1 | 15.7 | 20.5 |
| (hydr) | 517.4 | 2.0 | 75.7 | 79.5 |
| | 515.9 | 2.2 | 8.6 | 0 |
| 21.9 wt % V/SBA-15 | 518.8 | 1.9 | 33.9 | 37.2 |
| (dehydr) | 517.4 | 1.8 | 58.2 | 62.8 |
| | 515.9 | 2.2 | 7.9 | 0 |

Figure 8 depicts the XPS V/Si atomic ratios of the SBA-15-supported vanadia samples (see Table 2) as a function of the vanadium content in the bulk as determined by ICP. For comparison, the calculated V/Si bulk atomic ratios are shown as continuous line. The XPS V/Si values of the dehydrated V/SBA-15 samples closely follow their corresponding bulk values. In contrast, the XPS V/Si values of the hydrated V/SBA-15 samples show a deviation to smaller values with respect to their corresponding bulk values. This behavior is due to the significantly larger vanadia cluster size present in the hydrated sample as compared to the highly dispersed dehydrated sample. It can be explained by the fact that for cluster sizes exceeding those of the characteristic escape depth of the V2p electrons a smaller V signal and therefore a smaller V/Si ratio as that determined by ICP is observed.

## Discussion

**Changes in Vanadia Electronic Structure upon Dehydration.** On the basis of the literature data on V2p$_{3/2}$ binding energies,[39,40] the XP V2p$_{3/2}$ bands of the V/SBA-15 samples at 517.4 and 515.9 eV can readily be assigned to $V^{5+}$ and $V^{3+}$, respectively. It is evident that the band around 518.8 eV cannot solely be described by a change in oxidation state. However, final state effects are known to result in size-dependent BE shifts for small conducting particles on insulating substrates.[42] This is a result of the Coulomb interaction between the photoelectron and the positively charged particle. Such a situation applies to small vanadia particles with V ions in oxidation state 3+ and vanadyl groups at the surface, which are known to be formed under reduced-pressure conditions.[43] Therefore, our XPS results directly show that dehydration of the catalyst is accompanied by a strong decrease in cluster size, i.e., an increase in the dispersion of the catalyst.

The dispersion of the surface metal oxide species was studied by measuring the XPS vanadium to support cation intensity ratio. The V/Si intensity ratio was evaluated by using empirically derived atomic sensitivity factors (see Table 3).[28] Theoretical studies have shown that the XPS active phase to support cation ratio can be used to predict the volume ratio of a monolayer catalyst in case the wall thickness of the support is the same or smaller than the escape depth.[44] The thickness of the silica walls in case of our SBA-15 samples is estimated to be about 3 nm based on TEM, which is to be compared with the escape depth of a Silicon 2p electron of 3.8 nm (Mg K$\alpha$ radiation). As shown in Figure 8, a comparison of the V/Si XPS ratio of the dehydrated catalysts with the actual volume V/Si ratio of our catalyst as determined by ICP yields a surprisingly good agreement demonstrating the homogeneous distribution of vanadia throughout the sample. Thus, our XPS results give access to information about the catalysts composition, oxidation state distribution and dispersion representative of the bulk and allow for a direct correlation with the results obtained from Raman spectroscopy. The lower V/Si ratio of the hydrated compared to the dehydrated samples can be ascribed to the presence of hydrated $V_2O_5$ species forming clusters of significantly larger size as in case of the highly dispersed dehydrated samples (see discussion below).

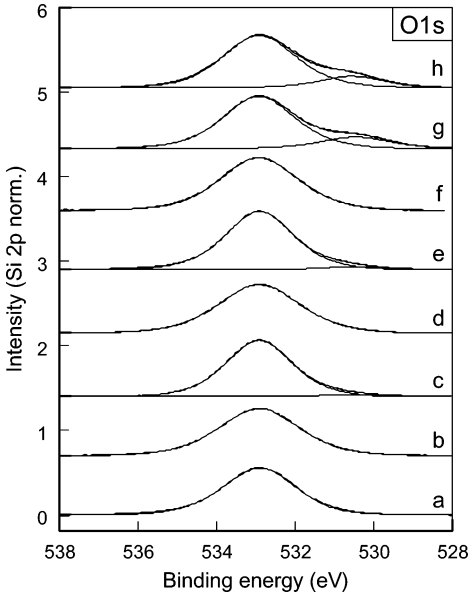


**Figure 7.** XP O1s spectra of (a) hydrated SBA-15, (b) dehydrated SBA-15, (c) hydrated 5.4 wt % V/SBA-15, (d) dehydrated 5.4 wt % V/SBA-15, (e) hydrated 10.8 wt % V/SBA-15, (f) dehydrated 10.8 wt % V/SBA-15, (g) hydrated 21.9 wt % V/SBA-15, and (h) dehydrated 21.9 wt % V/SBA-15, together with the least-square fits to the data. The spectra are offset for clarity. For details see text.

**TABLE 5: Results of the O1s Analysis of SBA-15- and SBA-15-Supported Vanadium Oxides**

| | position (eV) | width (eV) | % |
|---|---|---|---|
| SBA-15 (hydr) | 532.9 | 2.4 | 100 |
| SBA-15 (dehydr) | 532.9 | 2.6 | 100 |
| 5.4 wt % V/SBA-15 (hydr) | 532.9 | 2.2 | 96.4 |
| | 530.5 | 2.6 | 3.6 |
| 5.4 wt % V/SBA-15 (dehydr) | 532.9 | 2.6 | 100 |
| 10.8 wt % V/SBA-15 (hydr) | 532.9 | 2.2 | 95.9 |
| | 530.5 | 1.9 | 4.1 |
| 10.8 wt % V/SBA-15 (dehydr) | 532.9 | 2.6 | 100 |
| 21.9 wt % V/SBA-15 (hydr) | 532.9 | 2.4 | 82.7 |
| | 530.5 | 2.3 | 17.3 |
| 21.9 wt % V/SBA-15 (dehydr) | 532.9 | 2.4 | 83.3 |
| | 530.6 | 2.1 | 16.7 |

**Quantification of the Ratio of Highly Dispersed Vanadia and $V_2O_5$.** It is well-known that Raman cross sections, among other factors determining the resonance state, strongly depend on the degree of crystallinity of the studied material. Therefore, it is highly desirable to correlate Raman spectroscopy with a

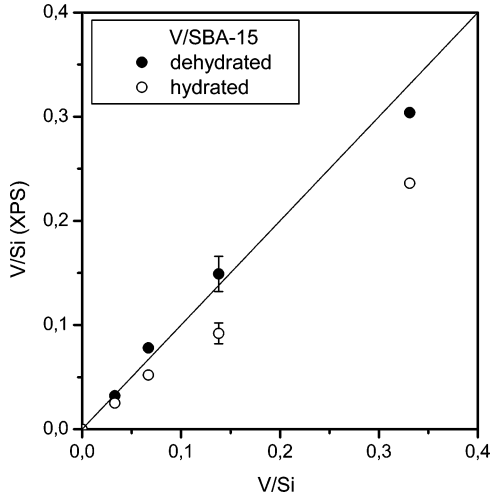


**Figure 8.** V/Si XP intensity ratio of dehydrated (filled) and hydrated (open) V/SBA-15 as a function of V loading expressed as V/Si. The bulk V/Si ratio is shown as continuous line.

technique such as XPS, which can differentiate and quantify the species of interest. Based on our XPS $V2p_{3/2}$ results for 21.9 wt % V/SBA-15, the ratio of vanadium in highly dispersed vanadia species and in bulk $V_2O_5$ is determined to be 0.59. As demonstrated above, the $V2p_{3/2}$ signal at 517.4 eV can be completely ascribed to bulk $V_2O_5$ due to the correlation of the $V2p_{3/2}$ with the corresponding O1s signal at 530.5 eV. Integration of the Raman peak around 1039 $cm^{-1}$ and the Raman peak at 994 $cm^{-1}$ yield a ratio of 0.22. Based on these results, at 514 nm excitation the Raman cross section for the V═O vibration of bulk $V_2O_5$ is estimated to be 3 times larger than that for highly dispersed vanadia species present at 21.9 wt % V/SBA-15. For 10.8 wt % V/SBA-15, the corresponding ratio of Raman intensities of highly dispersed vanadia and bulk $V_2O_5$ is determined as 10.65. A lower limit for the ratio of Raman cross sections for the V═O vibration of $V_2O_5$ and highly dispersed vanadia of 10.8 wt % V/SBA-15 can be estimated based on XP O1s results considering the following observations. The O1s emission of 10.8 wt % V/SBA-15 does not show a contribution of oxygen from $V_2O_5$. Simulations show that the presence of 2% (or more) of the O1s emission at 530.5 eV should be clearly noticeable in the spectrum. This suggests a ratio (per vanadium) of highly dispersed species and crystalline $V_2O_5$ of at least 49. Therefore, a lower limit for the ratio of Raman cross sections for the V═O vibration of $V_2O_5$ and highly dispersed vanadia of 4.6 is obtained. This is consistent with the experimentally determined value of 10 obtained previously for a 12 wt % $V_2O_5/SiO_2$ sample using laser excitation at 532 nm.[4] Similar to 10.8 wt % V/SBA-15, this sample contained only a small amount of $V_2O_5$. In addition, based on the UV−vis data the small difference in excitation wavelengths (532 nm vs 514 nm) is not expected to affect the above values. In conclusion, the discussion clearly shows that the ratio of Raman cross sections for the V═O vibrations at 994 and 1039 $cm^{-1}$ depends on the vanadium loading, i.e., the ratio of highly dispersed vanadia and crystalline $V_2O_5$ present in the sample. Therefore, its determination has to be treated with great care.

**Correlation of Changes in Dispersion and Structure.** The Raman results suggest that the hydrated state resembles a water-containing vanadia gel ($V_2O_5 \cdot nH_2O$). Upon dehydration, a dramatic change in molecular structure from pseudo-octahedrally to tetrahedrally coordinated monolayer-type vanadium oxide is observed as inferred from the Raman and UV−vis results.[18,20] The analysis of the XPS results shows that upon treatment in oxygen, the hydrated vanadia gel, which exhibits characteristics of $V_2O_5$-like polyvanadate species (BE: 517.4 eV) partly transforms into highly dispersed vanadium oxide (BE: 518.8 eV) with a significantly smaller ensemble size as evidenced by the increase in the intensity ratio of the 518.8 and 517.4 eV peak. The extent of this transformation is strongly dependent on the treatment conditions. Treatment in 20% $O_2$/He flow (50 mL/min) at 300 °C turned out to be much more efficient for the dehydration process than treatment in 200 mbar oxygen, i.e., treatment at the same partial pressure but in batch mode, and was therefore used throughout the study. Table 3 shows that the amount of highly dispersed species formed during dehydration depends on vanadium loading. Our results suggest that for lower loaded samples such as 2.7 wt % V/SBA-15 and 5.4 wt % V/SBA-15 it is more difficult to transform the water-containing vanadia gel completely into highly dispersed vanadia species. For comparison, in case of 10.8 wt % V/SBA-15 about 97% of the vanadia were transformed into highly dispersed species. Importantly, the band at 518.8 eV also contributes to the $V2p_{3/2}$ emission of all hydrated samples, which indicates that water from ambient significantly reduces the dispersion of part but not all of the surface vanadium oxide species. This is an important result as it demonstrates the sensitivity of XPS to detect even small changes in the dispersion of vanadia catalysts. In contrast, Raman appears to be insensitive to detect the simultaneous presence of both the highly dispersed and the much less dispersed state of the vanadium oxide surface species, which indicates that with the latter technique we see only part of the system. Thus, XPS yields important information on changes in catalyst dispersion, which is complementary to the information obtained from Raman spectroscopy.

## Conclusions

X-ray photoelectron spectroscopy (XPS) and Raman spectroscopy were combined within one experimental setup allowing for a direct correlation of XPS and Raman results. The potential of this setup is demonstrated in a study on the influence of water on the dispersion and structure of silica SBA-15-supported vanadia model catalysts. XPS characterization reveals that the $V2p_{3/2}$ emission consists of two contributions, which are assigned to vanadia with distinctly different cluster size. Dehydration by treatment in oxygen flow at elevated temperatures leads to a significant increase in total intensity and a substantial redistribution of spectral weight to higher binding energies as a result of a significant increase in the vanadia dispersion. The V/Si XPS intensity ratio of the dehydrated samples closely follows the corresponding bulk ratio over the whole range of vanadium loadings studied, which allows for a quantification of Raman-related features such as the relative cross sections of the vanadyl surface species. As water is omnipresent in partial oxidation reactions, unraveling the strong influence of water on the structure and dispersion of supported metal oxide catalysts is an important step toward a detailed understanding of the mode of operation of these catalyst systems.

**Acknowledgment.** The authors like to thank Gisela Lorentz for performing the BET measurements, Oksana Storcheva for performing the EPR experiments, and Ute Wild for technical assistance with the XPS setup. The authors are grateful to Robert Schlögl for fruitful discussions and continuous support of the project. The work is supported by SFB 546 of the Deutsche Forschungsgemeinschaft (DFG). C.H. thanks the DFG for providing an Emmy Noether fellowship.

## References and Notes


(1) Centi, G.; Cavani, F.; Trifiro, F. *Selective Oxidation by Heterogeneous Catalysis*; Kluwer Academic/Plenum Publishers: New York, 2000.

(2) Gryzbowska-Swierkosz, B. *Top. Catal.* **2000**, *11/12*, 23.

(3) Schraml-Marth, M.; Wokaun, A.; Pohl, M.; Krauss, H. L. *J. Chem. Soc., Faraday Trans.* **1991**, *87*, 2635.

(4) Xie, S.; Iglesia, E.; Bell, A. T. *Langmuir* **2000**, *16*, 7162.

(5) Gao, X.; Bare, S. R.; Weckhuysen, B.; Wachs, I. E. *J. Phys. Chem. B* **1998**, *102*, 10842 and references therein.

(6) Keller, D. E.; Koningsberger, D. C.; Weckhuysen, B. *J. Phys. Chem. B* **2006**, *110*, 14313.

(7) Venkov, T. V.; Hess, C.; Jentoft, F. C. *Langmuir* **2007**, *23*, 1768.

(8) Magg, N.; Immaraporn, B.; Giorgi, J. B.; Schroeder, T.; Bäumer, M.; Döbler, J.; Wu, Z.; Kondratenko, E.; Cherian, M.; Baerns, M.; Stair, P. C.; Sauer, J.; Freund, H.-J. *J. Catal.* **2004**, *226*, 88.

(9) Oyama, S. T.; Went, G. T.; Lewis, K. B.; Bell, A. T.; Somorjai, G. A. *J. Phys. Chem.* **1989**, *93*, 6786.

(10) Venezia, A. M. *Catal. Today* **2003**, *77*, 359.

(11) Inumaru, K.; Misono, M.; Okuhara, T. *Appl. Catal., A* **1997**, *149*, 133.

(12) Bond, G. C.; Zurita, J. P.; Flamerz, S. *Appl. Catal.* **1986**, *27*, 353.

(13) Nag, N. K.; Massoth, F. E. *J. Catal.* **1990**, *124*, 127.

(14) Gil-Llambias, F. J.; Escudey, A. M.; Fierro, J. L. G.; Lopez Agudo, A. *J. Catal.* **1985**, *95*, 520.

(15) Horvath, B.; Strutz, J.; Geyer-Lippmann, J.; Horvath, E. G. *Z. Anorg. Allg. Chem.* **1981**, *483*, 205.

(16) Dutoit, D. C. M.; Schneider, M.; Fabrizioli, P.; Baiker, A. *J. Mater. Chem.* **1997**, *7*, 271.

(17) Wark, M.; Koch, M.; Brückner, A.; Grünert, W. *J. Chem. Soc., Faraday Trans.* **1998**, *94*, 2033.

(18) Hess, C.; Schlögl, R. *Chem. Phys. Lett.* **2006**, *432*, 139.

(19) Tinnemans, S. J.; Mesu, J. G.; Kervinen, K.; Visser, T.; Nijhuis, T. A.; Beale, A. M.; Keller, D. A.; van der Eerden, A. M. J.; Weckhuysen, B. M. *Catal. Today* **2006**, *113*, 3 and references therein.

(20) Hess, C.; Hoefelmeyer, J. D.; Tilley, T. D. *J. Phys. Chem. B* **2004**, *108*, 9703.

(21) Hess, C.; Wild, U.; Schlögl, R. *Microporous Mesoporous Mater.* **2006**, *95*, 339 and references therein.

(22) Hess, C. *Surf. Sci.* **2006**, *600*, 3695.

(23) Hess, C.; Looi, M. H.; Abd Hamid, S. B.; Schlögl, R. *Chem. Comm.* **2006**, 451.

(24) Hess, C.; Drake, I. J.; Hoefelmeyer, J. D.; Tilley, T. D.; Bell, A. T. *Catal. Lett.* **2005**, *105*, 1.

(25) Thüne, P. C.; Verhagen, C. P. J.; van der Boer, M. J. G.; Niemantsverdriet, J. W. *J. Phys. Chem. B* **1997**, *101*, 8559 and references therein.

(26) van Hardevelt, R. M.; Gunter, P. L. J.; van Ijzendoorn, L. J.; Wielraaijer, W.; Kuipers, E. W.; Niemantsverdriet, J. W. *Appl. Surf. Sci.* **1995**, *84*, 1367.

(27) Barr, T. L. *Modern ESCA*; CRC Press: Boca Raton, FL, 1994.

(28) Briggs, D.; Seah, M. P. *Practical Surface Analysis*; Wiley: Chichester, U.K., 1990.

(29) Brinker, C. J.; Kirkpatrick, R.; Tallant, D. R.; Bunker, B. C.; Montez, B. *J. Non-Cryst. Solids* **1988**, *99*, 418.

(30) (a) Tallant, D. R.; Bunker, B. C.; Brinker, C. J.; Balfe, C. A. *Mater. Res. Soc. Symp. Proc.* **1986**, *73*, 261. (b) Stolen, R. H.; Walrafen, G. E. *J. Chem. Phys.* **1976**, *64*, 2623. (c) Brinker, B. C.; Tallant, D. R.; Roth, E. P.; Ashley, C. S. *Mater. Res. Soc. Symp. Proc.* **1986**, *61*, 387.

(31) The presence of a vanadia-related band at 1073 $cm^{-1}$ was confirmed by preliminary UV−Raman experiments in collaboration with Peter Stair.

(32) MacMillan, P. *Am. Mineral.* **1986**, *69*, 622.

(33) Abello, L.; Husson, E.; Repelin, Y.; Lucazeau, G. *J. Solid State Chem.* **1985**, *56*, 379.

(34) The spectra of Abello et al. in ref 33 were recorded at 647 nm excitation. Preliminary spectra of some of our samples taken at 632 nm excitation are in excellent agreement with those of Abello et al.

(35) Referring to the Si2p signal at 103.6 eV ($SiO_2$) the charging correction is <0.5 eV for V/$SiO_2$/Si.

(36) Gross, T.; Ramm, M.; Sonntag, H.; Unger, W.; Weijers, H. M.; Adem, E. H. *Surf. Interface Anal.* **1992**, *18*, 59.

(37) Treatment in 20% $O_2$/He flow (50 mL/min) at 300 °C turned out to be much more efficient for the dehydration process than treatment in 200 mbar oxygen at 300 °C (batch mode). Therefore, the former process was adopted throughout this study.

(38) The width of the contribution centered at 515.9 eV was fixed to 2.2 eV.

(39) Sawatzky, G. A.; Post, D. *Phys. Rev. B* **1979**, *20*, 1546.

(40) Eberhardt, M. A.; Proctor, A.; Houalla, M.; Hercules, D. M. *J. Catal.* **1996**, *160*, 27 and references therein.

(41) Dupuis, A.-C.; Abu Haija, M.; Richter, B.; Kuhlenbeck, H.; Freund, H.-J. *Surf. Sci.* **2003**, *539*, 99.

(42) Wertheim, G. K. *Z. Phys. B* **1987**, *66*, 53.

(43) Guimond, S.; Abu Haija, M.; Kaya, S.; Lu, J.; Weissenrieder, J.; Shaikhutdinov, S.; Kuhlenbeck, H.; Freund, H.-J.; Döbler, J.; Sauer, J. *Top. Catal.* **2006**, *38*, 117.

(44) Kerkhof, F. P. J. M.; Moulijn, J. A. *J. Phys. Chem. B* **1979**, *83*, 1612.